Supplementary information

Unveiling the restricted mobility of carbon nanotubes inside a long chain branched polymer matrix via probing the shear flow effects to the rheological and electrical properties of the filled systems

Jixiang Li[1], Abderrahim Maazouz[1,2], Khalid Lamnawar[1,*]

[1]Univ Lyon, CNRS, UMR 5223, Ingénierie des Matériaux Polymères, INSA Lyon, Université Claude Bernard Lyon 1, Université Jean Monnet, CEDEX, F-69621 Villeurbanne, France

[2]Hassan II Academy of Science and Technology, Rabat 10100, Morocco

*Correspondence: khalid.lamnawar@insa-lyon.fr (K.L.)

S0. Differential scanning calorimetry (DSC) of PPC and PPH

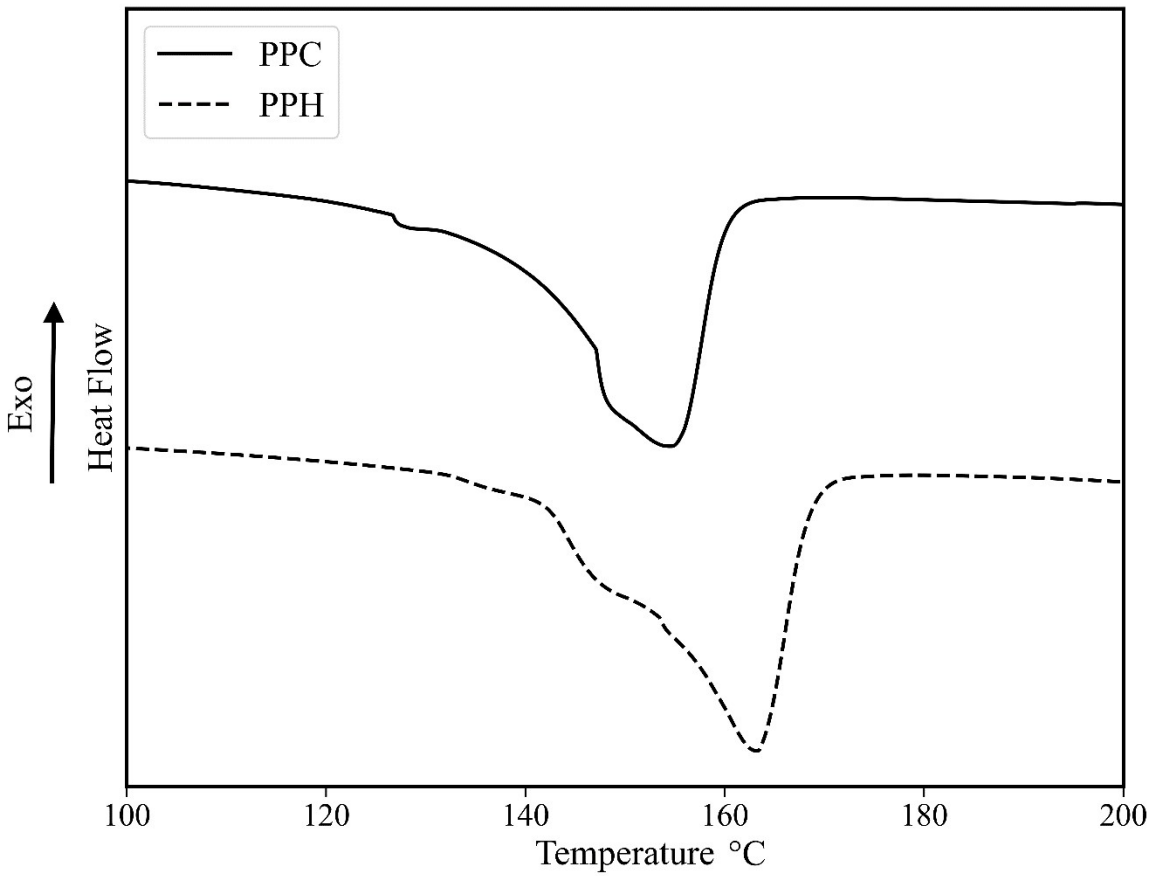

Figure S0 DSC first heating scans (10 °C/min) for Neat PPC (T_m = 154 °C) and PPH (T_m = 162 °C).

S1. The conductivity measurement

The electrical results were obtained from the measurement of the AC complex conductivity ($\sigma^*(\omega)$) as a function of frequency. The relationship between the AC complex conductivity and the complex permittivity is reflected in equation (1):

$$\sigma^*(\omega) = i\omega\varepsilon_0\varepsilon^*(\omega) \tag{1}$$

Here, ω is the frequency, ε_0 is the vacuum permittivity and ε*(ω) is the complex permittivity which includes the contributions of the electrical conductivity and can be expressed as:

$$\varepsilon^*(\omega) = \varepsilon'(\omega) - i\varepsilon''_{toal} = \varepsilon'(\omega) - i\left(\varepsilon''_P(\omega) + \frac{\sigma}{\omega\varepsilon_0}\right) \tag{2}$$

where $\varepsilon'(\omega)$ is the real part of the complex permittivity, ε''_{toal} is the total imaginary part, $\varepsilon''_P(\omega)$ represents the imaginary part of the permittivity due to the polarization phenomena, and σ is an electrical conductivity. By combining these two equations, we obtain:

$$\sigma^*(\omega) = i\omega\varepsilon_0\varepsilon^*(\omega) = i\omega\varepsilon_0\left(\varepsilon'(\omega) - i\left(\varepsilon''_P(\omega) + \frac{\sigma}{\omega\varepsilon_0}\right)\right) = \sigma + \omega\varepsilon_0\varepsilon''_P(\omega) + i\omega\varepsilon_0\varepsilon'(\omega) \tag{3}$$

where the real part of the complex conductivity is:

$$\sigma'(\omega) = \sigma + \omega\varepsilon_0\varepsilon''_P(\omega) \tag{4}$$

The equipment measured the total imaginary part—ε''_{toal} since the device could not distinguish between the two contributions. Accordingly, the electrical conductivity could not be formally isolated. However, since it did not increase with frequency, unlike the contribution from $\varepsilon''_P(\omega)$, the occurrence of a low-frequency plateau in the plot of $\sigma'(\omega)$ as a function of frequency indicates that the value of the electrical conductivity dominated the real part of the complex conductivity that then became very close to the true DC conductivity at low frequencies. The electrical conductivity values presented in this work for detecting the percolation refer to the value of $\sigma'(\omega)$ at the lowest frequency (20Hz).

S2. LCB information of PPH

More concrete evidence can be obtained by calculating the viscosity branching index g', the average number of branched points B_n and the LCB frequency λ. These values were plotted versus the molecular weight, as shown in Figure S1 and Figure S2. The values of B_n and λ between molecular weights of 3×10^4 and 1×10^6 g/mol are listed in Table S1. Although no great amount of LCBs was detected in PPH, there was already a significant influence on the viscoelastic properties compared with PPC with a linear chain structure.

Table S1 Long-chain branching characteristics. Viscosity branching index, average LCB per molecule and average branching frequency per 1000 units for PPH between 3×10^4 and 1×10^6 g/mol.

	g’	B_n (LCB/molecule)	λ (LCB/1000 monomers)
PPH	0.67	1.73	1.50

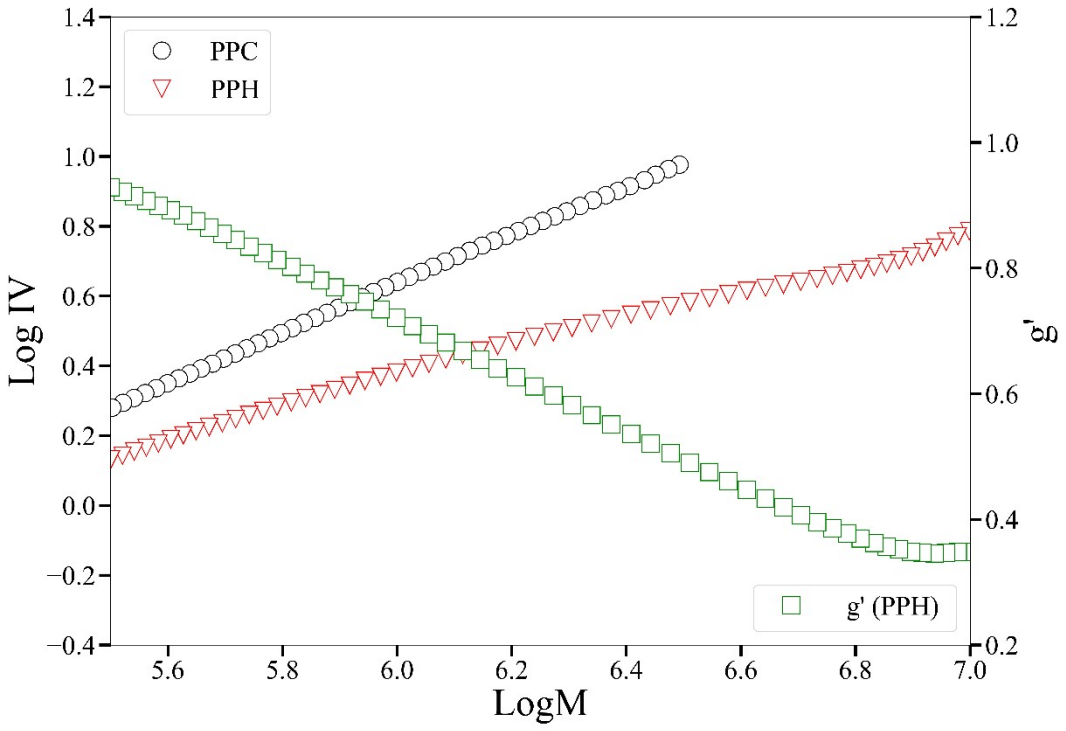

Figure S1 Intrinsic viscosity of PPC and PPH where g’ is the viscosity branching index.

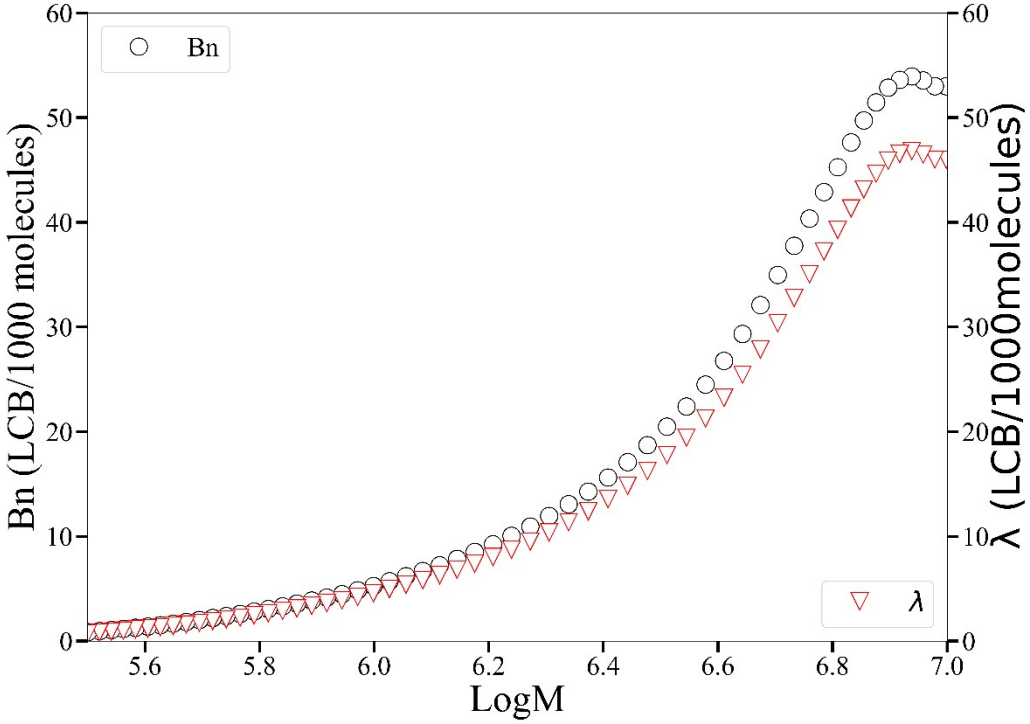

Figure S2 Average number of branch points per molecule Bn and long chain branching (LCB) frequency per 1000 monomer units λ for PPH.

S2. Rheology data of two PPs and their nanocomposites

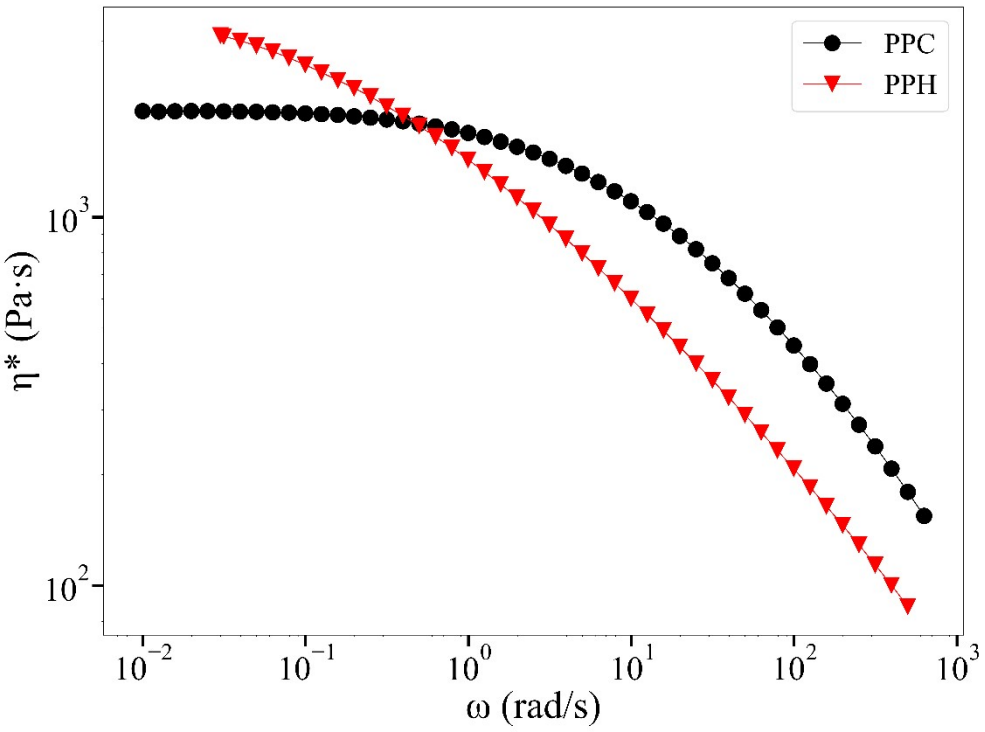

Figure S3 Complex viscosity of PPC and PPH at 200 °C

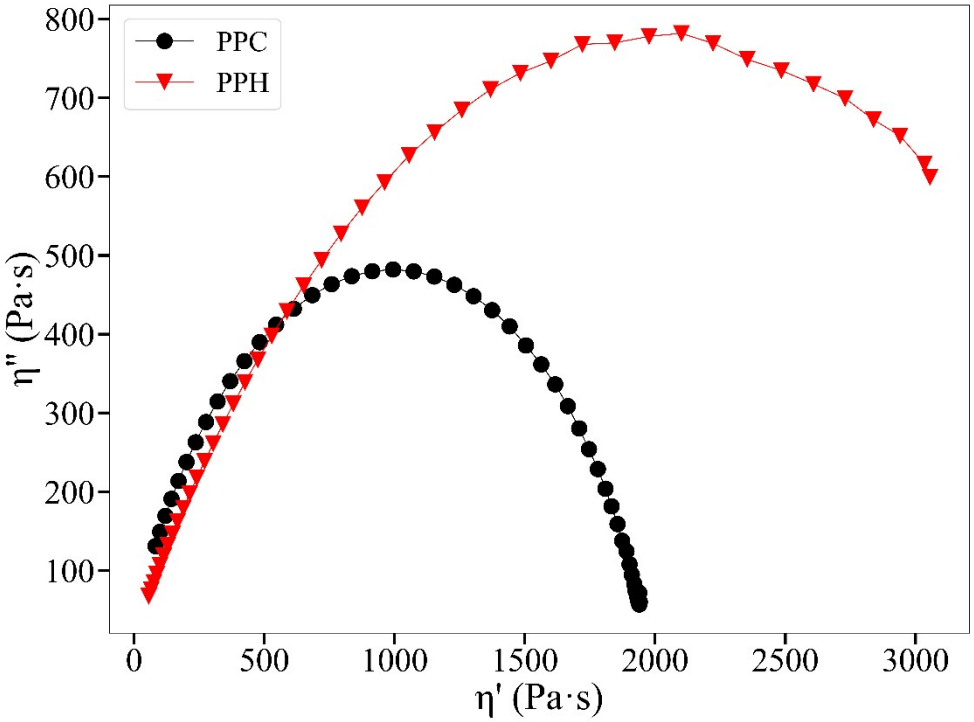

Figure S4 Cole-Cloe plots of neat PPC and PPH at 200 °C

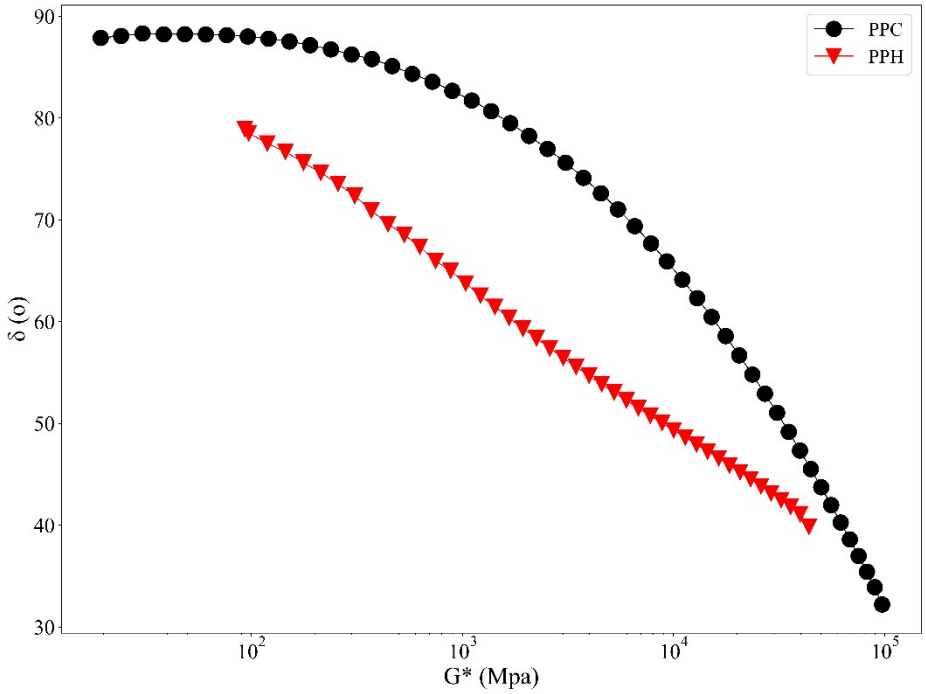

Figure S5 Complex modulus versus phase angle of neat PPC and PPH at 200 °C

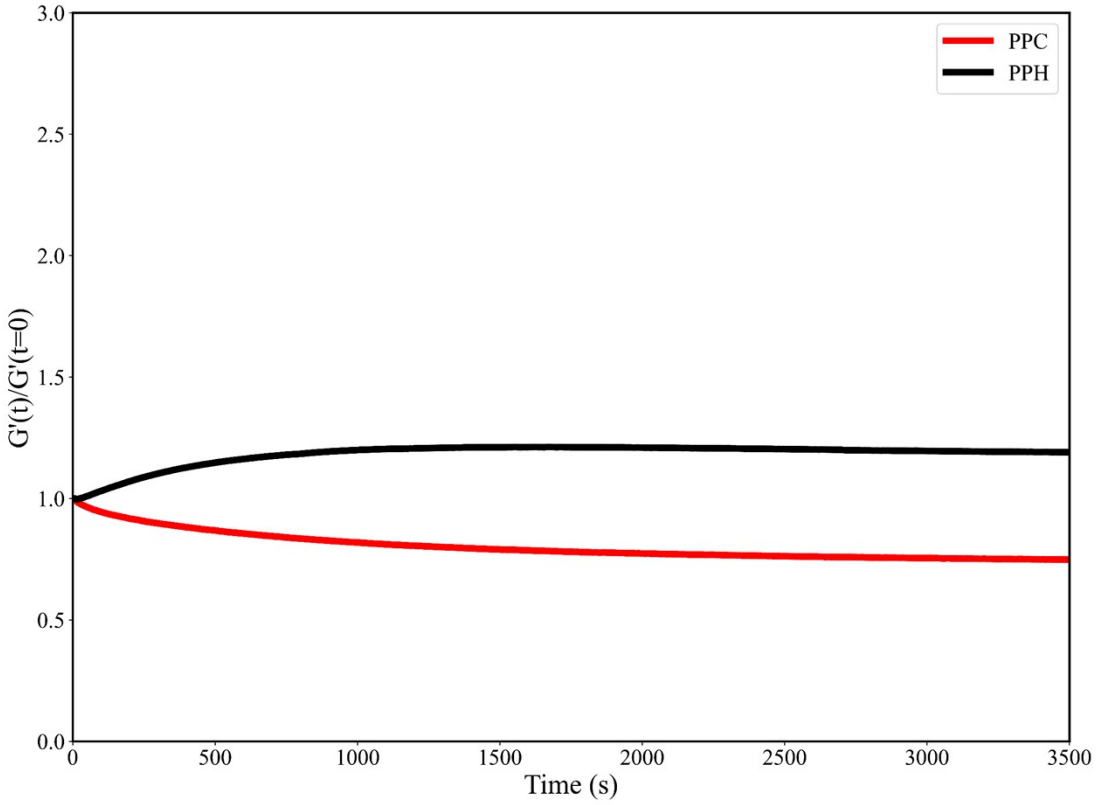

Figure S6 Dynamic time sweep of PPC and PPH which reflect the thermal stability of the used neat polymers are well.

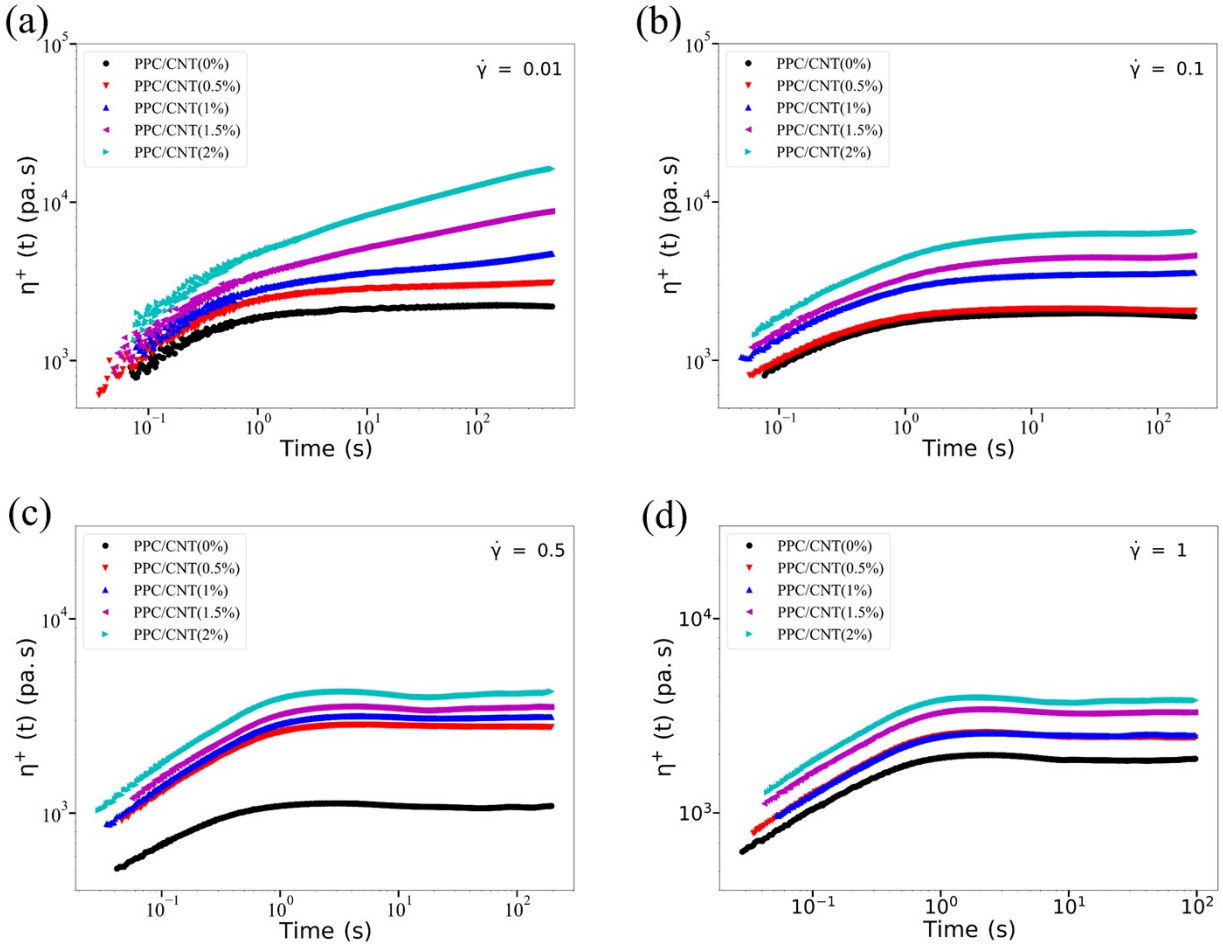

Figure S7 Start-up shear data of PPC and its nanocomposites with a shear rate of (a) 0.01 s^{-1}, (b) 0.1 s^{-1}, (c) 0.5 s^{-1} and (d) 1 s^{-1} at 200°C.

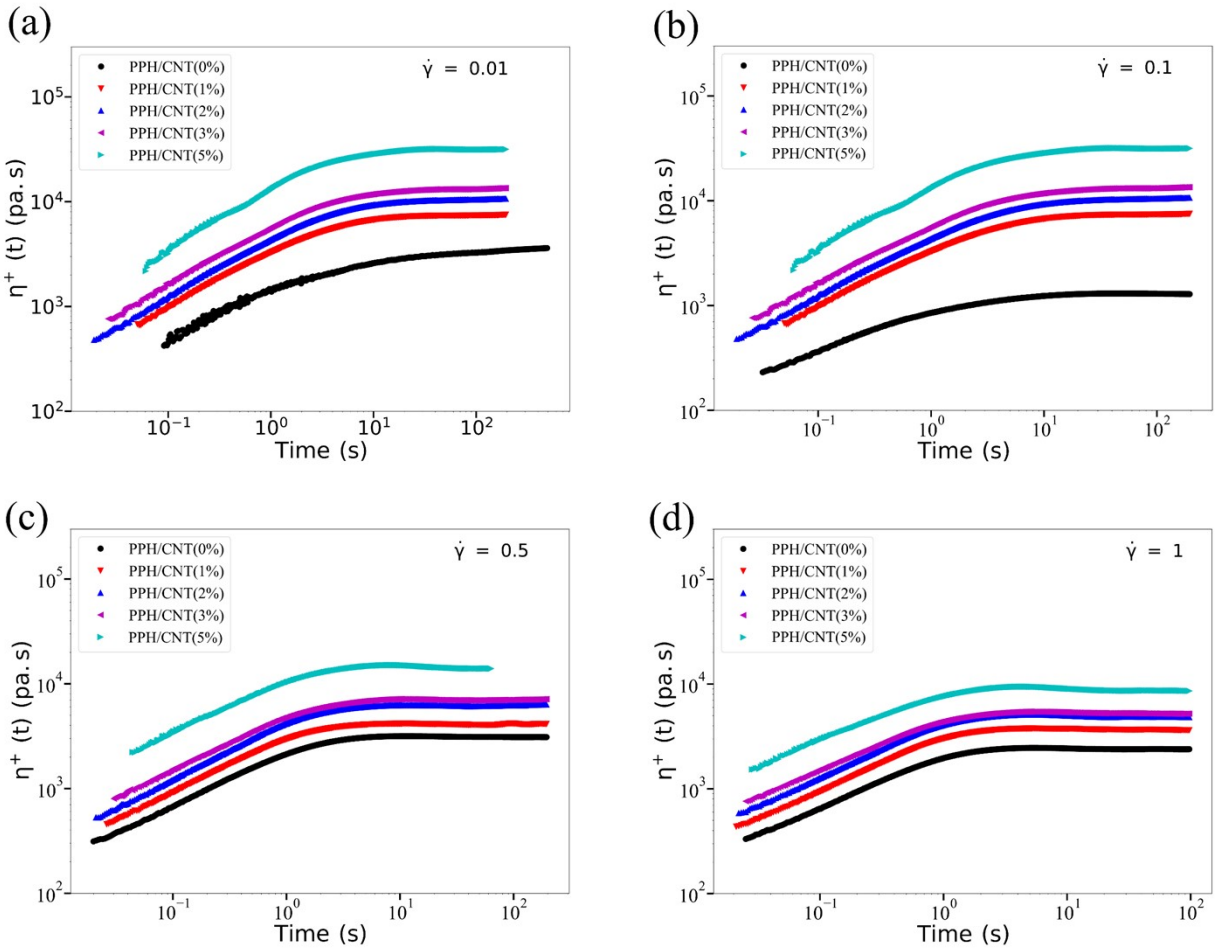

Figure S8 Figure S6 Start-up shear data of PPH and its nanocomposites with a shear rate of (a) 0.01 s^{-1}, (b) 0.1 s^{-1}, (c) 0.5 s^{-1} and (d) 1 s^{-1} at 200 °C

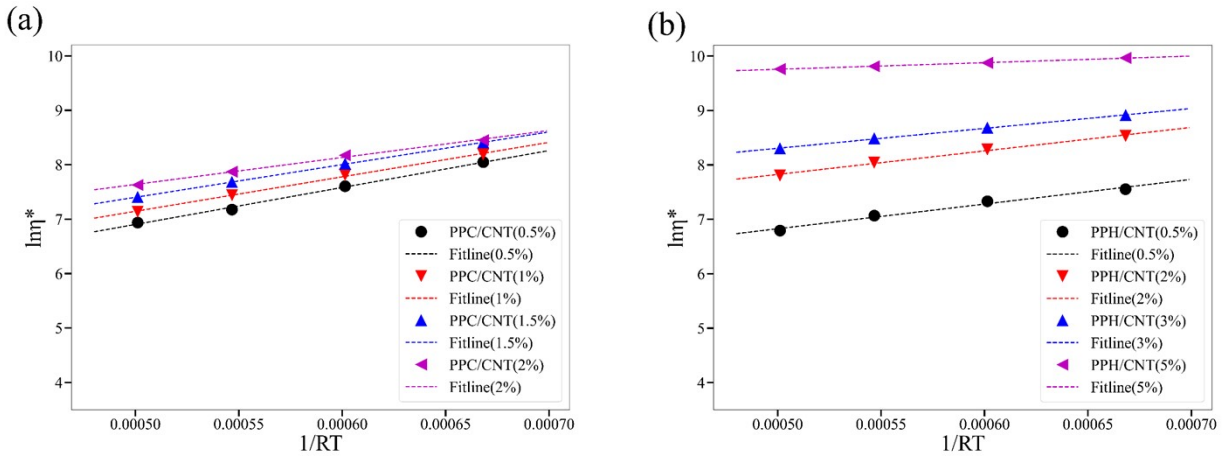

Figure S9 Plots of $\ln\eta^*$ vs $1/RT$ for PPC and PPH nanocomposites and the linear fitting lines.